Motion de-blurring by second-order intensity-correlated imaging

Zunwang Bo (薄遵望), Wenlin Gong (龚文林)*, and Shensheng Han (韩申生)

Key Laboratory for Quantum Optics and Center for Cold Atom Physics of CAS, Shanghai Institute of Optics and Fine Mechanics, Chinese Academy of Sciences, Shanghai 201800, China

**Corresponding author: gongwl@siom.ac.cn*

Received March 2, 2016; accepted May 16, 2016; posted online June 16, 2016

For a Hanbury Brown and Twiss system, the influence of relative motion between the object and the detection plane on the resolution of second-order intensity-correlated imaging is investigated. The analytical results, which are backed up by experiments, demonstrate that the amplitude and mode of the object's motion have no effect on the second-order intensity-correlated imaging and that high-resolution imaging can be always achieved by using a phase-retrieval method from the diffraction patterns. The use of motion de-blurring imaging for this approach is also discussed.

OCIS codes: 030.6600, 100.3010, 110.2990, 110.6150.
doi: 10.3788/COL201614.070301.

For conventional imaging, which is based on first-order correlation of a light field, relative motion between the object and the detection system will lead to the degradation of the imaging resolution. With the decrease in the imaging signal-to-noise ratio, the usual method to alleviate the motion blur effect is to shorten the exposure time. Since the laser was invented, a strategy that proved helpful to overcome the motion blur is to illuminate the object of interest with a parallel coherent light and to detect the object's Fourier patterns using an $f-f$ optical system[1]. For this strategy, because the Fourier patterns are insensitive to the relative motion between the object and the detection system, the object's images with high spatial resolution can be obtained by using a phase-retrieval method[2,3]. However, a strictly parallel coherent light, especially with a large illumination area, is hard to achieve in practice. For a divergent light source illuminating the object, phase differences will cause shifts of the Fourier patterns, which also lead to motion blurring for a moving object[1]. Recently, utilizing high-order correlation of a light field, the motion blur caused by the relative motion between an object and the detection system can be removed by using a method called ghost imaging, even while using a divergent incoherent light source for illumination[4–15]. Because the schematic of a Hanbury Brown and Twiss (HBT) system is also based on high-order correlation of a light field and is similar to the setup of ghost imaging, it is possible to realize motion de-blurring imaging[16]. However, compared with ghost imaging, the structure of the HBT is simpler, and it has a higher precision in optical measurements. In this Letter, we firstly theoretically analyze the influence of the relative motion between the object and the detection system on second-order intensity-correlated imaging for an HBT system in the far field. Then, the corresponding experimental demonstration is implemented and the images in the spatial domain are restored by Fienup's iterative phase-retrieval algorithm. Finally, we present a discussion on this approach and its potential future applications.

Figure 1 presents an experimental schematic of motion de-blurring imaging for an HBT system in the far field. The pseudo-thermal light source is formed by passing a laser beam of wavelength $\lambda = 532$ nm through a rotating ground glass disk[3–7,17]. The light propagates a distance z and then goes through an object. The object is placed on a motion platform, and the platform is driven by a stepper motor so it can move in one transverse dimension. The light field transmitted through the object is transformed into the far field by an $f-f$ optical system and then recorded by a CCD camera at the plane D_t. In addition, the stepping accuracy of the platform is 5 μm and the stepper motor is connected to a computer, which can control the object's motion.

For the optical system shown in Fig. 1, the impulse response function $h(\xi, u)$ between the source plane D_s and the detection plane D_t is time dependent, due to the

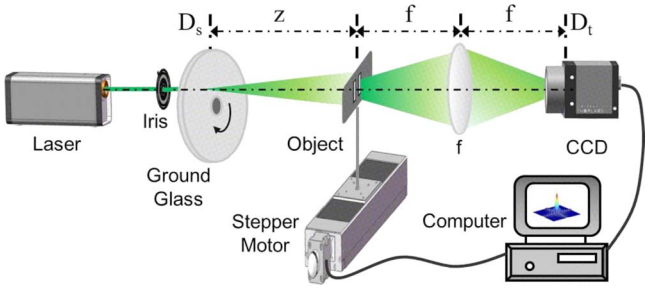

Fig. 1. Experimental schematic of motion de-blurring by second-order intensity-correlated imaging with pseudo-thermal light. A variable iris, which can continuously change the diameter of the laser beam from 1 to 12 mm, is placed in front of the ground glass disk. The object is driven by a stepper motor and moves one dimension perpendicular to the optical axis.

movement of the object. If the object's center position deviates η from the optical axis at time t, then the object's transmission function will be changed from $T(x)$ into $T(x-\eta(t))$, thus $h(\xi,u)$ can be expressed as

$$h(\xi,u,t) \propto \int \mathrm{d}x \exp\left\{\frac{jk}{2z}(x-u)^2\right\} \times T(x-\eta(t)) \exp\left\{-\frac{jk}{f}\xi x\right\}, \quad (1)$$

where μ and ξ are the coordinates in the source plane and detection plane, respectively. $T(x)$ denotes the transmission function of the object, and $k = 2\pi/\lambda$.

Based on the optical coherence theory[18], the second-order intensity-correlation function at the detection plane can be written as

$$\begin{aligned} G^{(2,2)}(\xi_1,\xi_2) &= \langle I_1(\xi_1) I_2(\xi_2)\rangle \\ &= \left\langle \int \mathrm{d}u_1 \mathrm{d}u_1' \mathrm{d}u_2 \mathrm{d}u_2' S(u_1) S^*(u_1') S(u_2) S^*(u_2') \right. \\ &\quad \left. \times h_1(\xi_1,u_1) h_1^*(\xi_1,u_1') h_2(\xi_2,u_2) h_2^*(\xi_2,u_2') \right\rangle \\ &= \int \mathrm{d}u_1 \mathrm{d}u_1' \mathrm{d}u_2 \mathrm{d}u_2' \langle S(u_1) S^*(u_1') S(u_2) S^*(u_2')\rangle \\ &\quad \times \langle h_1(\xi_1,u_1) h_1^*(\xi_1,u_1') h_2(\xi_2,u_2) h_2^*(\xi_2,u_2')\rangle, \end{aligned} \quad (2)$$

where we have assumed that the statistics of the source and the propagation regimes are independent. $I_1(\xi_1)$ and $I_2(\xi_2)$, respectively, are the intensity distribution and the intensity at the fixed position ξ_2, which is recorded by the same CCD at the detection plane D_t. $S(u)$ is the light field of the source, and $\langle\cdot\rangle$ denotes the ensemble average of a function.

Suppose the light field on the ground glass plane is fully spatially incoherent and the intensity distribution is uniform as a constant intensity I_0. Then,

$$\langle S(u) S^*(u')\rangle \propto I_0 \delta(u-u'), \quad (3)$$

where $\delta(x)$ is the Dirac delta function.

According to statistical optics, the correlation function of the intensity fluctuation is[19]

$$\Delta G^{(2,2)}(\xi_1,\xi_2) = \langle I_1(\xi_1) I_2(\xi_2)\rangle - \langle I_1(\xi_1)\rangle\langle I_2(\xi_2)\rangle. \quad (4)$$

If the source's spatial incoherence at the object plane is satisfied according to Eq. (9) of Ref. [20], by substituting Eqs. (1)–(3) into Eq. (4) and supposing the field fluctuations obey a complex circular Gaussian random process with a zero mean, after some calculations, we have

$$\begin{aligned} \Delta G^{(2,2)}(\xi_1,\xi_2) &\propto \left\langle \left| \mathcal{F}\left\{ \left| T\left(\frac{2\pi}{\lambda f}(\xi_1-\xi_2)\right)\right|^2 \right\} \right. \right. \\ &\quad \left. \left. \times \exp\left\{\frac{jk}{f}(\xi_1-\xi_2)\eta(t)\right\}\right|^2 \right\rangle \\ &\propto \left| \mathcal{F}\left\{ \left| T\left(\frac{2\pi}{\lambda f}(\xi_1-\xi_2)\right)\right|^2 \right\}\right|^2, \end{aligned} \quad (5)$$

where $\mathcal{F}\{\cdots\}$ denotes the Fourier transform of a function. From Eq. (5), we can see that the diffraction patterns obtained by second-order intensity-correlated imaging with pseudo-thermal light is independent of η, regardless of whether η is random, deterministic, time varying, or none of those. It is also observed that the center of the diffraction patterns will move with the position ξ_2. If we set $\xi_2 = 0$, then Eq. (5) can be rewritten as

$$\Delta G^{2,2}(\xi_1,\xi_2=0) \propto \left| \mathcal{F}\left\{ \left| T\left(\frac{2\pi}{\lambda f}\xi_1\right)\right|^2 \right\}\right|^2. \quad (6)$$

From Eq. (6), when the source's illumination region on the object plane is larger than the motion amplitudes of the object and satisfies homogeneous statistical distribution, the relative motion between the object and the detection plane will not lead to the blurring of diffraction patterns for second-order intensity-correlated imaging with pseudo-thermal light. Therefore, the object's amplitude-dependent image with high resolution can be always reconstructed from the diffraction patterns if a phase-retrieval method is used.

A platform experiment based on the optical system shown in Fig. 1 was performed to demonstrate the theoretical results. The experimental parameters are set as follows: $z = 600$ mm, $f = 50$ mm, and the effective transmission aperture of the lens is $L = 25.4$ mm. The object is a double slit, with silt width $a = 40$ μm, center-to-center separation $d = 120$ μm, and slit height $h = 800$ μm. The object, driven by a stepper motor, moves in a transverse dimension, and the motion speed of the target driven by the stepper motor is 32 μm/s. In order to verify the theoretical results, the exposure time window for the CCD camera should be short enough so that the recorded speckle is clear for each sampling. In the experiment, the exposure time window for the CCD camera is set to be 30 μs and the sampling frequency is 10 Hz, which means that the target only moves 1 nm and can be considered to be static for each sampling. The pixel size of the CCD camera is 6.9 μm × 6.9 μm. The images recorded by using the CCD camera are 430 × 170 pixels, and the number of measurements for the reconstruction of the second-order intensity-correlated imaging is 8000. In the process of image reconstruction, the fixed coordinate is set in the center of the image recorded by the CCD camera, and we have used the intensity fluctuation correlation reconstruction algorithm[21]. The influences of both the motion amplitudes and motion modes on the resolution of second-order intensity-correlated imaging are experimentally demonstrated.

Figure 2 presents the results of second-order intensity-correlated imaging in different motion amplitudes, where the motion mode obeys a uniform statistical distribution and the transmission aperture of the iris is set as $D = 4.0$ mm. The results of the corresponding second-order intensity-correlated imaging are shown in Fig. 2(a)–2(e), respectively, when the maximum motion amplitude deviating from the optical axis is set as 0, 500, 1000, 2000, and 4000 μm. Based on Fienup's iterative phase-retrieval algorithm[2], the object's images in the spatial domain, as displayed in the upper right corners of Figs. 2(a)–2(e), can be directly retrieved from the diffraction patterns. In the process of the phase-retrieval algorithm, the phase-dependent part of the object is supposed to be a constant, while the amplitude-dependent part is limited by the prior information of the object's size. Under these constraint conditions, a series of increasingly accurate results can be obtained by iterative transform b etween the Fourier domain and spatial domain, and this iterative process has been proven to be convergent in mathematics. It is observed that the imaging resolution does not degrade upon increasing the motion amplitude for the approach of second-order intensity-correlated imaging, which is consistent with the theoretical analysis described by Eqs. (5) and (6). For comparison, we remove the rotating ground glass disk shown in Fig. 1, and the transmission aperture of the iris is set as $D = 12.0$ mm.

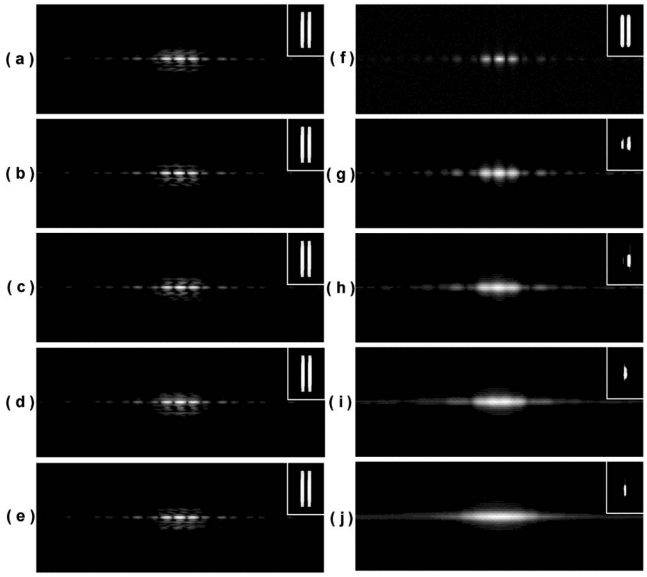

Fig. 2. Experimental results in different motion amplitudes and motion modes obey uniform statistical distribution (averaged 8000 measurements). (a)–(e) are the diffraction patterns achieved by second-order intensity-correlated imaging when the maximum motion amplitudes deviating from the optical axis are 0, 500, 1000, 2000, and 4000 μm, respectively. (f)–(j) are the corresponding results of conventional Fourier imaging, which is performed by removing the rotating ground glass disk shown in Fig. 1. The upper right corner is the image in the spatial domain recovered by using a phase-retrieval algorithm from the corresponding diffraction pattern.

The results of conventional Fourier imaging with coherent light with the corresponding motion amplitudes are illustrated in Figs. 2(f)–2(j), using the same experimental parameters as the second-order intensity-correlated imaging. From Figs. 2(f)–2(j), as the motion amplitude is increased, the object's imaging resolution will be dramatically decreased for conventional Fourier imaging techniques. As known to all, if the object is set to move in the horizontal direction, motion blurring should not have an influence on the resolution in the vertical direction. However, the real situation of the experiment is that the motion path of the object is not to strictly parallel to the horizontal direction and there is a little vibration in the vertical direction when the object moves. Therefore, the resolutions of Figs. 2(g)–2(j) in the vertical direction also have little degradation.

Compared with uniform motion, imaging of random moving objects is more meaningful in applications. Figures 3(a)–3(c) show the statistical distributions of different motion modes when the motion amplitude is set as 2000 μm. The corresponding diffraction patterns obtained by second-order intensity-correlated imaging and the images in the spatial domain restored by Fienup's iterative phase-retrieval algorithm are displayed in Figs. 3(d)–3(f). Similar to the results shown in Figs. 2(b)–2(e), the motion modes have no effect on the imaging resolution of second-order intensity-correlated imaging, which is in agreement with the analytical results.

According to the Klyshko's pictures[22], the imaging process for the HBT system shown in Fig. 1 can be

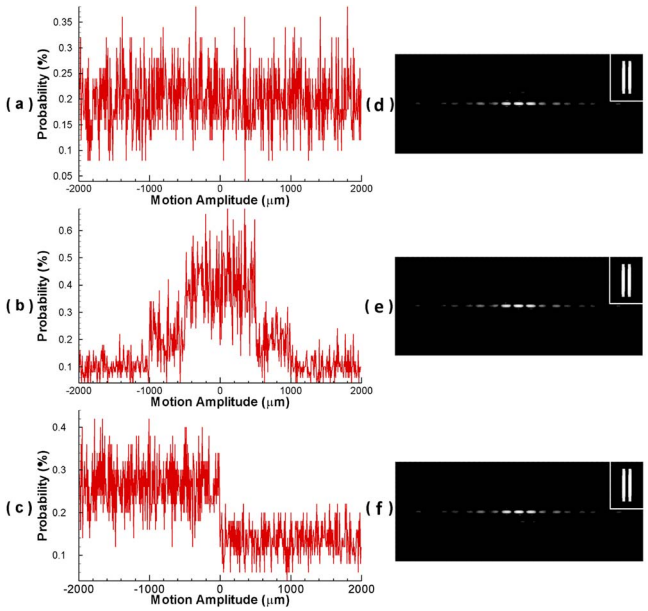

Fig. 3. Experimental results in different motion modes and the maximum motion amplitude deviating from the optical axis is 2000 μm (averaged 8000 measurements). (a)–(c) are the probability distributions of the motion modes. (d)–(f) display the diffraction patterns achieved by second-order intensity-correlated imaging and the reconstructed images in spatial domain are shown in the upper right corner.

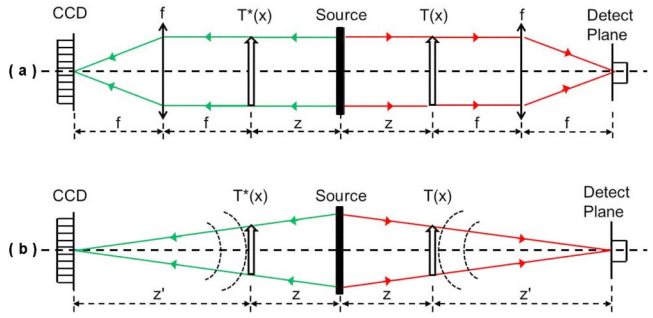

Fig. 4. Explanation of motion de-blurring imaging for an HBT system. (a) The explanation for the schematic shown in Fig. 1, and (b) the explanation for a standard lensless HBT setup. The source shown in Fig. 1 acts as a phase-conjugated mirror.

explained as follows: by the reversibility of the light field, a point-like source emitting light from the detection plane (namely, one pixel of the CCD camera), as displayed in Fig. 4(a), is firstly collimated by a lens with focal length f and then illuminates the object $T(x)$. Since the pseudo-thermal light source acts as a phase-conjugated mirror[23], photons transmitted from the object $T(x)$ are reflected by the source to the object $T^*(x)$. Then, the information of $T(x)T^*(x)$ is transformed into the far field by an $f-f$ optical system, and we can obtain the object's Fourier-transform diffraction patterns at the CCD camera plane. It is observed that Fig. 4(a) corresponds to the case of illuminating an object $T(x)T^*(x)$ with a parallel coherent light and detecting the object's diffraction patterns in the Fourier plane; thus, the object's motion does not lead to the movement of diffraction patterns, and high-resolution imaging can be always obtained when the effective transmission aperture of the lens f is larger than the object's motion amplitudes. What is more, the resolution of the diffraction patterns obtained by intensity correlation is also similar to the case of parallel coherent illumination in Fig. 4(a), which is that the optical resolution is determined by the aperture of lens f[24]. Although we only give the demonstration of motion de-blurring imaging for an HBT system with a lens in the far field, the approach is easy to expand to the lensless HBT setup shown in Fig. 4(b). In Fig. 4(b), even if a spherical wave emitted from a point-like source illuminates the object and the CCD camera is located in the Fresnel area, thanks to the property of phase conjugation, the phase retardation of the quadratic terms at the planes of $T(x)$ and $T^*(x)$ are cancelled out by each other, which is equivalent to an imaging process of illuminating an object $T(x)T^*(x)$ with a parallel coherent light and detecting the object's information in the far field. Therefore, a lensless HBT setup can also overcome the motion blur caused by the relative motion between the object and the detection system. However, if the object is illuminated by a non-uniform source, the intensity distribution of the diffraction patterns can still be achieved but with a little distortion, so a uniform illumination may be helpful for the diffraction patterns. This approach can be very useful to the imaging of moving objects in the wavebands without coherent sources and lenses, such as the x ray band.

In conclusion, for an HBT system, both a theoretical analysis and an experimental demonstration prove that the diffraction patterns obtained by second-order intensity-correlated imaging are insensitive to the relative motion between the object and the detection plane; thus, an imaging with a high spatial resolution can be always reconstructed by using a phase-retrieval algorithm. This technique provides a useful approach to overcome the motion blurring caused by random, high-frequency shaking.

This work was supported by the National 863 Program of China (No. 2013AA122901), the National Natural Science Foundation of China (No. 61571427), and the Youth Innovation Promotion Association CAS (No. 2013162).

References

1. J. W. Goodman, *Introduction to Fourier Optics* (Mc Graw-Hill, 1968).
2. V. Elser, J. Opt. Soc. Am. A **20**, 40 (2003).
3. M. Zhang, Q. Wei, X. Shen, Y. Liu, H. Liu, J. Cheng, and S. Han, Phys. Rev. A **75**, 021803 (2007).
4. D.-Z. Cao, J. Xiong, and K. Wang, Phys. Rev. A **71**, 013801 (2005).
5. M. D. Angelo and Y. H. Shih, Laser Phys. Lett. **2**, 567 (2005).
6. A. Gatti, M. Bache, D. Magatti, E. Brambilla, F. Ferri, and L. A. Lugiato, J. Mod. Opt. **53**, 739 (2006).
7. W. Gong, P. Zhang, X. Shen, and S. Han, Appl. Phys. Lett. **95**, 071110 (2009).
8. J. H. S. A. R. W. Boyd, Quantum Inf. Process. **11**, 949 (2012).
9. C. Zhang, W. Gong, and S. Han, Chin. J. Lasers **39**, 1214003 (2012).
10. C. Zhang, W. Gong, and S. Han, Appl. Phys. Lett. **102**, 021111 (2013).
11. E. Li, Z. Bo, M. Chen, W. Gong, and S. Han, Appl. Phys. Lett. **104**, 251120 (2014).
12. X. Li, C. Deng, M. Chen, W. Gong, and S. Han, Photon. Res. **3**, 153 (2015).
13. L. Wu, Y. Zhang, L. Cao, N. Zhao, J. Wu, and Y. Zhao, Chin. Opt. Lett. **10**, 122802 (2012).
14. D. Duan, S. Du, L. Yan, S. Jiang, Y. Liu, L. Zhang, and Y. Xia, Chin. Opt. Lett. **12**, 072701 (2014).
15. A. Zhang, W. Li, L. Zhao, H. Ye, Y. Liu, X. Wei, and Z. Wang, Chin. Opt. Lett. **12**, 052701 (2014).
16. R. H. Brown and R. Q. Twiss, Nature **177**, 27 (1956).
17. X. Xu, E. Li, X. Shen, and S. Han, Chin. Opt. Lett. **13**, 071101 (2015).
18. R. J. Glauber, Phys. Rev. **130**, 2529 (1963).
19. J. W. Goodman, *Statistical Optics* (Wiley, 1985).
20. W. Gong and S. Han, J. Opt. Soc. Am. B **27**, 675 (2010).
21. W. Gong and S. Han, Phys. Lett. A **374**, 1005 (2010).
22. D. N. Klyshko, *Photons and Nonlinear Optics* (Gordon and Breach, 1988).
23. A. Valencia, G. Scarcelli, M. D'Angelo, and Y. Shih, Phys. Rev. Lett. **94**, 063601 (2005).
24. H. Liu, J. Cheng, and S. Han, J. Appl. Phys. **102**, 103102 (2007).